International Journal of Biological Macromolecules 278 (2024) 135041

Contents lists available at ScienceDirect

International Journal of Biological Macromolecules

journal homepage: www.elsevier.com/locate/ijbiomac

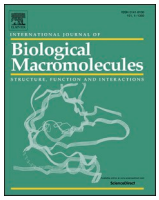

Proteogenomics-guided functional venomics resolves the toxin arsenal and activity of *Deinagkistrodon acutus* venom

Ignazio Avella [a,b,c,*,1], Lennart Schulte [a,b,c,d,1], Sabine Hurka [c,d,e], Maik Damm [a,b,c], Johanna Eichberg [d,f], Susanne Schiffmann [c,g], Marina Henke [c,g], Thomas Timm [h], Günther Lochnit [h], Kornelia Hardes [c,d,f], Andreas Vilcinskas [b,c,d], Tim Lüddecke [a,c,d,**]

[a] *Animal Venomics Lab, Fraunhofer Institute for Molecular Biology and Applied Ecology (IME), Ohlebergsweg 12, 35392 Giessen, Germany*
[b] *Institute for Insect Biotechnology, Justus Liebig University Giessen, Heinrich-Buff-Ring 26–32, 35392 Giessen, Germany*
[c] *LOEWE Centre for Translational Biodiversity Genomics (LOEWE-TBG), Natural Product Genomics, Senckenberganlage 25, 60325 Frankfurt am Main, Germany*
[d] *Branch for Bioresources, Fraunhofer Institute for Molecular Biology and Applied Ecology (IME), Ohlebergsweg 12, 35392 Giessen, Germany*
[e] *BMBF Junior Research Group in Bioeconomy (BioKreativ) "SymBioÖkonomie", Ohlebergsweg 12, 35392 Giessen, Germany*
[f] *BMBF Junior Research Group in Infection Research "ASCRIBE", Ohlebergsweg 12, 35392 Giessen, Germany*
[g] *Fraunhofer Institute for Translational Medicine and Pharmacology (ITMP), 60596 Frankfurt am Main, Germany*
[h] *Protein Analytics, Institute of Biochemistry, Faculty of Medicine, Justus Liebig University Giessen, Friedrichstrasse 24, 35392 Giessen, Germany*

ARTICLE INFO

Keywords:
Proteomics
Cytotoxicity
Snakebite

ABSTRACT

Snakebite primarily impacts rural communities of Africa, Asia, and Latin America. The sharp-nosed viper (*Deinagkistrodon acutus*) is among the snakes of highest medical importance in Asia. Despite various studies on its venom using modern venomics techniques, a comprehensive understanding of composition and function of this species' venom remains lacking. We combined proteogenomics with extensive bioactivity profiling to present the first genome-level catalogue of *D. acutus* venom proteins and their exochemistry. Our analysis identified an unusually simple venom containing 45 components from 20 distinct protein families. Relative toxin abundances indicate that C-type lectin and C-type lectin-related protein (CTL), snake venom metalloproteinase (svMP), snake venom serine protease (svSP), and phospholipase A_2 (PLA_2) constitute 90 % of the venom. Bioassays targeting key aspects of viperid envenomation showed considerable concentration-dependent cytotoxicity, particularly in kidney and lung cells, and potent protease and PLA_2 activity. Factor Xa and thrombin activities were minor, and no plasmin activity was observed. Effects on haemolysis, intracellular calcium (Ca^{2+}) release, and nitric oxide (NO) synthesis were negligible. Our analysis provides the first holistic genome-based overview of the toxin arsenal of *D. acutus*, predicting the molecular and functional basis of its life-threatening effects, and opens novel avenues for treating envenomation by this highly dangerous snake.

1. Introduction

Snakebite is a neglected tropical disease recognised by the World Health Organization (WHO) [1]. It affects an estimated 1.2 to 5.4 million people annually, resulting in up to approximately 140,000 deaths and 400,000 reported cases of long-term disabilities worldwide [2–5]. This disease primarily impacts rural, economically disadvantaged communities in Sub-Saharan Africa, Asia, and Latin America [2,6,7]. Due to the challenge of collecting reliable data from the remote settings where snakebite often occurs, only a fraction of cases is reported, leading to a severe underestimation of its true global burden [4,8].

Acknowledging the global importance of this health risk, the WHO has set a strategic goal to halve the number of deaths and disabilities due to snakebite by 2030 [9]. A crucial element in achieving this goal is

* Correspondence to: I. Avella, Institute for Insect Biotechnology, Justus Liebig University Giessen, Heinrich-Buff-Ring 26–32, 35392 Giessen, Germany.
** Correspondence to: T. Lüddecke, Animal Venomics Lab, Fraunhofer Institute for Molecular Biology and Applied Ecology (IME), Ohlebergsweg 12, 35392 Giessen, Germany.
E-mail addresses: ignazio.avella@ime.fraunhofer.de (I. Avella), tim.lueddecke@ime.fraunhofer.de (T. Lüddecke).
[1] Shared first authorship.

https://doi.org/10.1016/j.ijbiomac.2024.135041
Received 21 July 2024; Received in revised form 20 August 2024; Accepted 22 August 2024
Available online 23 August 2024

developing a coherent understanding of the composition and effects of the venoms produced by snake species of major clinical relevance. This stems from the wide variety of symptoms that can arise following envenomation, which depend on diversity and abundance of the toxins present in snake venoms, as well as their molecular targets and enzymatic activities [3,10]. For instance, viper venoms tend to primarily cause coagulotoxicity and tissue damage through the action of phospholipases A_2, serine proteases, and metalloproteinases, commonly found in high amounts in them [11–14]. Resolving the venom compositions from medically relevant species, and understanding the structural features (i.e., sequence-based determinants of toxin bioactivity) of their toxin arsenals, as well as the symptoms they can cause, is thus crucial in guiding the development of therapeutic tools against snakebite and improving its treatment.

The rise of venomics, broadly defined as the application of different "omics" technologies to the study of toxic organisms, revolutionised venom research [15–17]. Especially through pioneering studies employing proteomics, venomics has enabled the exploration of a wide range of venom profiles from all across the animal kingdom, particularly in snakes [13,18,19]. In recent times, the application of proteomics to the study of snake venom has been further enhanced by an increasing body of works utilising transcriptomics and genomics [20–22]. The latter is particularly valuable for identifying and studying snake venom components. Indeed, it allows to infer the genomic localisation and synteny of venom proteins, and facilitates large-scale comparative evolutionary analyses [23–25]. From a pathobiochemical perspective, genomics is of pivotal importance because it resolves the primary structure of venom toxins at both the nucleic acid and amino acid levels, providing species-specific databases. Additionally, it allows the in silico investigation of structure-function relationships without the high error rates found in de novo transcriptomic analyses. However, to date, the undoubtedly powerful genomic toolkit has rarely been integrated with proteomics to study snake venom profiles, and the tremendous potential of such analyses in the context of snakebite remains largely untapped [24,25].

The sharp-nosed viper (*Deinagkistrodon acutus*) is a medically relevant pit viper (family Viperidae, subfamily Crotalinae) occurring in southern China, Taiwan, and northern Vietnam, and its presence has been suggested also for Laos [26–28] (Fig. 1). A thickset, powerful snake often exceeding 150 cm in total length [29], the sharp-nosed viper is able to inject remarkably high quantities of venom, reportedly up to 180 mg (dry weight) with a single bite [30]. Consequently, envenomation caused by *D. acutus* can be extremely severe, manifesting dramatic coagulotoxic and tissue-damaging symptoms that frequently lead to permanent morbidity or death [31–34]. Therefore, the sharp-nosed viper is considered of the highest medical importance across most of its distribution by the WHO [27].

Based on its high medical relevance, several studies have investigated individual toxins from *D. acutus* venom over the years [35–38]. More recently, first exploratory proteomic studies attempted to shed light on its composition, and revealed that C-type lectin and C-type lectin-related protein (CTL), snake venom metalloproteinase (svMP), serine proteases (svSP), and phospholipase A_2 (PLA_2) dominate the *D. acutus* venom profile [39–41]. The abundance of such toxins aligns with the predominantly coagulotoxic and cytotoxic symptoms of *D. acutus* envenoming [29,32,42]. Furthermore, multiple genomes and venom gland transcriptomes have been generated for this species, providing a basis for a more thorough exploration of its venom composition, as well as the molecular mechanisms behind the evolution of snake venom toxins and venom-related genes [43–45]. Nonetheless, despite the considerable amount of omics-derived data on *D. acutus*, this wealth of knowledge has yet to be fully utilised in venom research endeavours, and much remains to be learned about the toxin arsenal of this critically important snake.

In the present work, we leverage a recently sequenced high-quality genome of the sharp-nosed viper [44] alongside thorough proteomics analysis to provide a first comprehensive overview of its venom composition, and establish a full sequence-level atlas of its components. This proteogenomics-guided inventory (sensu Jaffe et al. [46] and Nesvizhskii [47]) of the *D. acutus* toxin arsenal is complemented by extensive bioactivity profiling on key viper venom targets to place the identified components within a functional context. Specifically, we assess the cytotoxicity and haemolytic activity of sharp-nosed viper venom, as well as the activity of protease, PLA_2, coagulation factor Xa, thrombin, and plasmin. Additionally, we test its impact on intracellular Ca^{2+} release, associated with processes like muscle contraction and synaptic transmission, and NO synthesis, a cellular response to stress and inflammation. Our study offers a detailed picture of the compositional

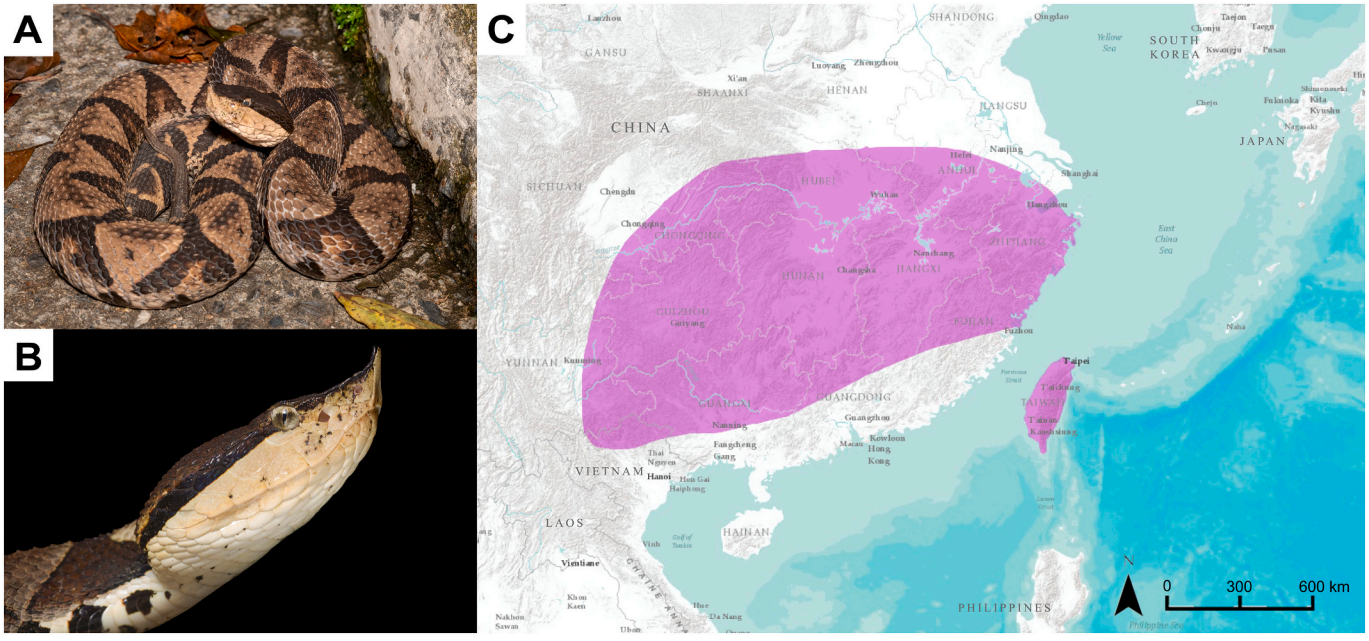

Fig. 1. Appearance and distribution range of the sharp-nosed viper (*Deinagkistrodon acutus*). (A) Full-body photograph and (B) close-up of adult *D. acutus*. (C) Distribution range of the species, sourced from the WHO Snakebite Information and Data Platform [27]. Photo credits: Sam Huang (A), Tom Williams (B).

diversity of *D. acutus* venom, the structure of its components, and a comprehensive assessment of its biological activities, thus serving as a valuable foundation for understanding and treating the symptoms resulting from bites inflicted by this species.

2. Materials and methods

2.1. Venom samples

Lyophilised *D. acutus* venom was purchased from Latoxan (https://www.latoxan.com/index.php) and stored at −20 °C until analysis. It comprised of pooled venom samples obtained from an unknown number of captive adult sharp-nosed vipers originating from mainland China.

2.2. Shotgun proteomics of D. acutus venom

To analyse the protein composition of *D. acutus* venom, we employed a mass spectrometry (MS) shotgun proteomics approach, following the procedure previously applied by our group [48,49]. Initially, 10 μg of lyophilised venom were dissolved in 25 mM ammonium bicarbonate with 0.6 nM ProteasMaxTM (Promega) and reduced with freshly prepared 5 mM dithiothreitol (DTT) for 30 min at 50 °C. Free thiols were alkylated with 10 mM iodoacetamide for 30 min in the dark at room temperature (24 °C). The reaction was quenched with excess cysteine (15 mM) and trypsin added at a 50:1 ratio and incubated for 16 h at 37 °C. The reaction was terminated by adding trifluoroacetic acid (TFA) to a final concentration of 1 % (*v*/v). Samples were purified using a C18-ZipTip (Millipore), dried under vacuum conditions, and reconstituted in 10 μl of 0.1 % TFA (*v*/v) in ddH_20.

For LC-MS analysis, 1 μg tryptic digested peptides in 0.1 % formic acid were initially separated using an UltiMate 3000RSLCnano system (Thermo Fisher Scientific) with a 50 cm μPAC C18 column (Pharma Fluidics) at 35 °C. Peptide elution was carried out in 0.05 % formic acid (*v*/v) using a linear gradient of MeCN, increasing from 3 % to 44 % (v/v) over 4 h at a flow rate of 300 nl/min, followed by washing the column with 72 % (v/v) MeCN. For MS analysis, eluting peptides were injected in positive mode by an Advion TriVersa NanoMate (Advion BioSciences) into an Orbitrap Eclipse Tribrid MS instrument (Thermo Fisher Scientific) with a spray voltage of 1.7 kV and a source temperature of 275 °C. MS/MS scans were performed in data-independent acquisition (DDA) mode. The instrument performed full MS scans every 2.5 s over a mass range of *m/z* 400–1600, with the resolution of the Orbitrap set to 120000. The RF lens was set to 30 %, auto gain control (AGC) was set to standard with a maximum injection time of 50 milliseconds (ms). In each cycle, the most intense ions (charge state 2–6) above a threshold ion count of 5000 were selected with an isolation window of 0.7 m/z for CID fragmentation at a normalised collision energy of 35 % and an activation time of 10 ms. Fragment ion spectra were acquired in the linear IT with a scan rate set to rapid and mass range to normal and a maximum injection time of 100 ms.

Data acquisition and analysis utilised Xcalibur v4.3.73.11 (Thermo Fisher Scientific) for instrumental operations, and Proteome Discoverer v2.5.0.400 (Thermo Fisher Scientific) for data processing.

For protein annotation, PEAKS Studio 11.0 (build 20230414; Bioinformatics Solutions Inc.) was utilised with the following settings: Parent Mass Error Tolerance (15.0 ppm), Fragment Mass Error Tolerance (0.5 Da), Precursor Mass Search Type (monoisotopic), Enzyme (Trypsin), Max Missed Cleavages (2), Digest Mode (Semi-Specific), Peptide Length Range (6–45). Post-translational modifications (PTMs) included carbamidomethylation (+57.02) as a fixed modification and various variable modifications: acetylation (K) (+42.01), Oxidation (M) (+15.99), pyro-glu from E (−18.01) and pyro-glu from Q (−17.03), with a maximum of two variable PTMs per peptide. The database search was conducted against the *D. acutus* genome published by Yin et al. [44], including Deep Learning Boost (Yes) and FDR Estimation (Enabled). For qualitative analysis, proteins were considered only if they met specific criteria: a Protein score −10lgP (≥15), a minimum of one unique peptide, and a Peptide-Spectrum Matches (PSM) FDR of 0.003, Peptide Sequence FDR of 0.01 and Protein Group FDR of 0.125.

An ultra-sensitive DIAMOND v3.5.2 [50] search was performed against UniProtKB/Swiss-Prot v2024_01 [51] (downloaded on 11 March 2024), UniProtKB/TrEMBL v2024_01 (downloaded on 11 March 2024), a combined database of UniProtKB/Swiss-Prot and UniProtKB/TrEMBL restricted to taxon ID 8570 (Serpentes, downloaded on 19 March 2024), VenomZone (https://venomzone.expasy.org; accessed on 11 March 2024) to identify venom components. The *E*-value was set to a maximum of 1×10^{-3} and max-target-seqs was set to 0 to search the entire database. For each DIAMOND hit, the coverage of query and subject was calculated. Similarity was calculated with the BLOSUM62 matrix [52] using BioPython v1.83 [53]. The results were sorted by bitscore, similarity, query and subject coverage in descending order for each venom candidate. The resulting top DIAMOND hit was used for further analysis. SignalP v6h [54] slow-sequential mode for Eukaryota was used to predict signal peptides. Additional screening using InterProScan v5.66–98.0 [55] included all databases. Components without a signal peptide and that could not be assigned to an InterProScan ID were removed from our data set. Based on all information collected, putative venom components were assigned to the appropriate toxin family/group.

In order to not only represent the diversity of *D. acutus* venom components but also provide information on toxin quantities, the relative abundances were calculated based on spectral counts (SpC), which can serve as a proxy of protein abundance [56,57]. The Normalized Spectral Abundance Factor (NSAF) of each protein was calculated, as presented below:

$$(\mathrm{NSAF})_k = \frac{(\mathrm{SpC}/L)_k}{\sum_{i=1}^{N}(\mathrm{SpC}/L)_i}$$

The NSAF for a protein *k* is calculated by normalising its SpC per its length (*L*), against the sum of all SpC/*L* for N proteins [58,59].

A detailed list of all identified venom components, as well as additional information on the calculated relative abundances, is reported in Tables S1–S4. Mass spectrometry proteomics data have been deposited under the project name “DATASET - Mass Spectrometry - Snake venom proteomics of *Deinagkistrodon acutus*” to the Zenodo repository (https://zenodo.org) with the dataset identifier “12785576” [60].

2.3. Reverse-phase high-performance liquid chromatography (RP-HPLC)

For the RP-HPLC analysis, 125 μg of lyophilised venom were diluted in double-distilled water (ddH_2O) containing 0.1 % TFA (*v*/v) and profiled with a ICS-300 SP HPLC system (Dionex) equipped with a C18 column (218TP, 3 μm, 50 × 4.6 mm, Vydac) operating with the following gradients with 0.1 % TFA (v/v) at a flowrate of 2 ml/min: 5 min initial phase (100 % ddH_2O), followed by a linearly increasing MeCN gradient (3 min 0–15 %, 15 min 15–45 %, 3 min 45–70 %), and 4 min at constant 70 % MeCN. Wavelength was observed at $\lambda = 280$ nm by a Ultimate 3000 Diode Array Detector (Dionex) with a scan rate of 0.2 s. Process control and data acquisition were performed with Chromeleon (version 6.80 SR11 Build 3160 (183147), Dionex). The venom chromatogram was cleared from background noise by subtracting a preliminary blank.

2.4. Gel electrophoresis (SDS-PAGE)

For one-dimensional SDS-PAGE profiling, 5 μg of lyophilised *D. acutus* venom were dissolved in ddH_2O, mixed with non-reducing or reducing (containing 5 % (*v*/v) 2-mercaptoethanol) Laemmli buffer. Subsequently, the sample was incubated at 95 °C for 5 min, before being loaded onto 4–20 % Mini-PROTEAN® TGX™ Precast Protein Gels (Bio-Rad). One-dimensional SDS-PAGE was carried out for 60 min at 150 V in

a Mini-PROTEAN® Tetra Vertical Electrophoresis Cell (Bio-Rad). A protein ladder (Precision Plus Protein All Blue Standard 10–250 kDa, Bio-Rad) was used as apparent molecular weight reference. Protein staining was the performed using ROTI®Blue quick solution (Carl Roth), destaining in ddH_2O. Digital images of the resulting gels were obtained using a Nikon D80 digital camera (Nikon).

2.5. Biological activity assays

2.5.1. Cytotoxicity

To assess the cytotoxicity of *D. acutus* venom, different assay workflows were applied. For the cytotoxicity assays performed on Madin-Darby canine kidney II (MDCK II) cells and the human alveolar basal epithelial cell line A549 (CLS Cell Lines Service), cells were maintained in Dulbecco's modified Eagle's medium (DMEM) GlutaMAX supplemented with 10 % foetal calf serum (FCS) and 1 % penicillin/streptomycin, and kept at 37 °C in a 5 % CO_2 atmosphere. Cytotoxicity assays were carried out following the protocol described by Hurka et al. [61]. Briefly, cells were seeded in 96-well plates and grown to confluence. The venom was dissolved in water, ionomycin (7.74 mg/ml stock, Cayman Chemicals) was dissolved in DMSO, and cells were treated with either venom (25, 2.5 or 0.25 μg/ml), ddH_2O (negative control), or ionomycin (100 μM, positive control) and incubated at 37 °C in a 5 % CO_2 atmosphere. After 48 h, cell viability was assessed by measuring the ATP content using the CellTiter-Glo Luminescent Cell Viability assay (Promega) according to the manufacturer's instructions. Luminescence was recorded using black 96-well plates in a Synergy H4 microplate reader (BioTek). Measurements were performed in triplicates, and expressed as mean ± standard deviation. Luminescence readings were normalised to the vehicle control (ddH_2O), which was set to 100 % cell viability.

Additional cytotoxicity assays were performed on the macrophage cell line RAW 264.7 and peripheral blood mononuclear cells (PBMCs), as well as human embryonic kidney cells (HEK 293T) and neuroblastoma cells SH-SY5Y, following the protocol described by Erkoc et al. [62]. Cell viability was assessed using the Orangu™ assay (Cell Guidance Systems). In summary, 2×10^5 cells from each tested cell line were placed in 96-well plates and exposed to different concentrations of *D. acutus* venom or ddH_2O as a control for 24 h. Subsequently, 10 μl of Orangu™ cell counting solution was added, followed by 60 min of incubation. Absorbance readings were taken at $\lambda = 450$ nm with a reference wavelength of $\lambda = 650$ nm using an EnSpire 2300 Multimode Plate Reader (Perkin Elmer). Cell viability was expressed as a percentage relative to the control cells treated with ddH_2O, which were considered 100 % viable. Celecoxib (100 μM) and ddH_2O were applied as positive control as negative control, respectively. For every cytotoxicity assay performed, 1 μl of treatment (i.e., venom, positive control, or negative control) was added to 99 μl of medium present in each well of the 96-well plates used.

2.5.2. Protease activity

To investigate the protease activity of *D. acutus* venom, we used a Protease Assay Kit (539,125, Sigma-Aldritch) following the manufacturer's manual, as described by Schulte et al. [49]. Briefly, the venom was diluted in ddH_2O to obtain three aliquots at different concentrations (200, 100, and 50 μg/ml). Triplicates of each concentration were subsequently tested against trypsin (final concentration of 166 μg/ml in PBS with 1.66 mg/ml bovine serum albumin, Calbiochem) and ddH_2O, used as positive and negative controls, respectively. In a round-bottom 96-well plate, a mixture containing 25 μl fluorescein thiocarbamoyl-casein derivatives (FTC-casein), 25 μl incubation buffer, and 10 μl of either venom or control was prepared. The plate was incubated at 37 °C and 120 rpm for 2 h. Afterward, 120 μl of trichloroacetic acid (5 % in ddH_2O, Carl Roth) was added to each well, and the plate further incubated for 20 min. The plate was then centrifuged at 4 °C and 500 × *g* for 15 min, followed by careful transfer of 40 μl of supernatant to a flat-bottom 96-well plate, where it was mixed with 160 μl of assay buffer. Absorbance at $\lambda = 492$ nm was measured using a BioTek Eon microplate reader and Gen v2.09 software. Mean absorbance values obtained from each treatment were normalised to positive controls (100 %) after subtraction of negative controls (0 %).

2.5.3. Phospholipase A_2 activity

To evaluate the phospholipase A_2 (PLA_2) activity of *D. acutus* venom, we used a EnzChek™ Phospholipase A_2 Assay Kit (E10217, Thermo Fisher), following the manufacturer's manual. The positive control was prepared by diluting the 500 Units/ml PLA_2 stock solution to 10 Units/ml in 1× PLA_2 reaction buffer. The negative control consisted of 1× PLA_2 reaction buffer without PLA_2. We then prepared the Lipid Mix by mixing together 30 μl 10 mM dioleoylphosphatidylcholine (DOPC), 30 μl 10 mM dioleoylphosphatidylglycerol (DOPG), and 30 μl 1 mM PLA_2 substrate. We then added 5 ml 1 × PLA_2 reaction buffer to a 20 ml beaker containing a small magnetic stir bar, and placed the beaker on a magnetic stirrer. To prepare 5 ml substrate-liposome for 100 assays, we slowly injected 50 μl of Lipid Mix into the side of the vortex in the beaker using a pipettor fitted with a narrow orifice gel-loading tip. Following Still et al. [63], we prepared venom pre-dilutions at five different concentrations (50, 25, 12.5, 6.25, and 3.125 μg/ml). Subsequently, 50 μl of the controls and 50 μl of each venom sample at different concentrations were injected into individual wells of a black 96-well plate (F-bottom), and added 50 μl of the substrate-liposome mix to each well to start the reaction. The plate was incubated at room temperature for 50 min, protected from light. Fluorescence was measured using a Synergy H4 microplate reader (BioTek) equipped for excitation at $\lambda = 470$ nm and fluorescence emission at $\lambda = 515$ nm. Measurements were normalised against the positive control (100 %) after subtraction of the negative control (0 %).

2.5.4. Haemolytic activity

To explore the haemolytic activity of *D. acutus* venom, we applied the protocol described by Sæbø et al. [64] with minor modifications. Briefly, we centrifuged 0.2 ml of sheep blood for 5 min at 804 × *g* at a temperature of 4 °C. We then washed the erythrocytes through the following steps: (i) removal of the supernatant by aspiration, (ii) addition of 1 ml of Alsever buffer, and (iii) resuspension of the pellet with a cut 1000 μl pipette tip to reduce shear forces. The washing was repeated until the supernatant was clear. After the final washing, the supernatant was removed and the remaining pellet diluted 1:100 (*w/v*) in Alsever buffer, in order to obtain a 1 % erythrocyte suspension. Subsequently, we added 50 μl of the 1 % erythrocyte suspension to each V-bottom well of a 96-well plate. We then prepared venom pre-dilutions at five different concentrations (40, 20, 10, 5, and 2.5 μg/ml) in Alsever buffer, and added 50 μl of each to the corresponding well with the 1 % erythrocyte suspension. We used 1 % Triton X-100 dilution as positive control and Alsever buffer as negative control, and added 50 μl of each to the corresponding well with the 1 % erythrocyte suspension. Each venom treatment and the controls were prepared in triplicates. The plate was incubated for 60 min at 37 °C and 130 RPM (Multitron, Infors HT). After incubation, the plates were centrifuged at 804 × *g* for 5 min at 4 °C, and 50 μl of the supernatant from each well were then transferred to a transparent, flat-bottom 96-well plate. Finally, absorbance at $\lambda = 405$ nm was measured in triplicates by a Synergy H4 microplate reader (BioTek) with the following parameters: shaking: double-orbital, frequency: second level, speed: slow, duration: 10 s. The obtained values were normalised to positive control (100 %) after subtraction of negative control (0 %).

2.5.5. Plasmin activity

Investigating the plasmin activity of *D. acutus* venom, we used the Plasmin Activity Assay Kit (MAK244, Sigma-Aldrich), following the manufacturer's manual. As a first step, 2 μl of Plasmin Substrate and 48 μl of Plasmin Assay Buffer were added to each well of a white, flat-

bottom 96-well plate. Furthermore, a 10 μg/ml stock solution of Plasmin Enzyme Standard in Plasmin Dilution Buffer was prepared to be used as positive control. The lyophilised venom was suspended in ddH_2O and pre-diluted in Plasmin Assay Buffer, and added to the substrate in triplicates (1:1), at concentrations of 50, 25, 12.5, 6.25, and 3.125 μg/ml. The pre-diluted stock for the positive control was further diluted in Plasmin Assay Buffer to be added at a concentration of 5 μg/ml, while 50 μl Plasmin Assay Buffer were added as negative control. After incubating for 55 min at 37 °C and protected from light, plasmin activity was measured in a Synergy H4 plate reader (H4MLFPTAD, BioTek), with excitation set to $\lambda = 360$ nm and fluorescence measured at $\lambda = 450$ nm. Measurements were normalised to positive control (100 %) after subtraction of negative control (0 %).

2.5.6. Thrombin activity

In order to assess the thrombin activity of *D. acutus* venom, we used the Thrombin Activity Fluorometric Assay Kit (MAK242, Sigma-Aldrich), following the manufacturer's manual. To prepare the substrate solution, 5 μl Thrombin Substrate were added to 45 μl Thrombin Assay Buffer in each well of a white, flat-bottom plate, protected from light. A stock of 2.5 μg/ml Thrombin enzyme standard in Thrombin Dilution Buffer was prepared as positive control. The lyophilised venom was suspended in ddH_2O and prediluted (1:5) in Thrombin Assay Buffer to be added in triplicates (1:1) to the substrate, at concentrations of 50, 25, 12.5, 6.25, and 3.125 μg/ml. The positive control stock was further diluted in Thrombin Assay Buffer and added to the plate in a concentration of 0.3 μg/ml, as well as 50 μl Thrombin Assay buffer as negative control. After incubation for 55 min at 37 °C, protected from light, thrombin activity was measured in a Synergy H4 plate reader (H4MLFPTAD, BioTek), with excitation set to $\lambda = 350$ nm and fluorescence measured at $\lambda = 450$ nm. Measurements were normalised to positive control (100 %) after subtraction of negative control (0 %).

2.5.7. Coagulation factor Xa activity

To evaluate the factor Xa (FXa) activity of *D. acutus* venom, we used the Factor Xa Activity Fluorometric Assay Kit (MAK238-1KT, Sigma-Aldrich), following the manufacturer's manual. The substrate solution was prepared by adding 2 μl FXa Substrate to 48 μl FXa Assay Buffer per well in a white, flat-bottom plate, protected from light. The positive control was prepared by diluting the FXa Enzyme Standard in FXa Dilution Buffer for a 5 μg/ml stock solution. The lyophilised venom was suspended in ddH_2O and prediluted (1:5) in FXa Assay Buffer to be added in triplicates (1:1) to the substrate, at concentrations of 50, 25, 12.5, 6.25, and 3.125 μg/ml. The pre-diluted positive control was further diluted in FXa Assay Buffer, and added to the plate in a concentration of 0.4 μg/ml, as well as 50 μl FXa Assay buffer as negative control. After incubation for 55 min at 37 °C and protected from light, FXa activity was measured in a Synergy H4 plate reader (H4MLFPTAD, BioTek), with excitation set to $\lambda = 350$ nm and fluorescence measured at $\lambda = 450$ nm. Measurements were normalised to positive control (100 %) after subtraction of negative control (0 %).

2.5.8. Assessment of intracellular Ca^{2+} levels

The intracellular release of calcium (Ca^{2+}) is induced by the activation of cell surface receptors, and takes place following several key cellular functions [65]. Quantification of Ca^{2+} release was performed by labelling cells with the calcium fluorescence probe Fluo-8-AM, as described by Erkoc et al. [62]. Briefly, 2×10^4 HEK 293T cells were plated in 96-well poly-D-lysine-coated plates and incubated at 37 °C for 24 h. Afterward, the cells were treated with 4.19 μg/ml Fluo-8-AM in Hanks' balanced salt solution (HBSS) for 1 h at 37 °C. Subsequently, the Fluo-8/HBSS solution was replaced with 100 μl of HBSS. Using an ImageXpress Micro confocal high-content imaging system (Molecular Devices), images were captured at a rate of five per second. For the induction assay, cells were exposed to vehicle (negative control), *D. acutus* venom, or 5 μM ionomycin (positive control, Sigma-Aldrich), and images were taken every second for 20 s. In the inhibition assay, 5 μM ionomycin was added to the venom-treated samples after 30 min, and images were captured similarly. Data analysis was performed using MetaXpress software. The fluorescence intensity threshold was established based on pre-treatment cells, and cells exhibiting a signal above this threshold were quantified. In the induction assay, the number of cells surpassing the threshold in venom-treated samples was compared with untreated samples. In the inhibition assay, venom-treated samples were compared with cells treated with ionomycin. Normalisation for the induction assay and the inhibition assay was performed against the positive control (100 %) and against the vehicle/negative control (100 %), respectively.

2.5.9. Assessment of NO levels

Nitric oxide (NO) in phagocytes is a component of the innate immune response to pathogens [66]. The ability of *D. acutus* venom to influence the synthesis of NO in RAW 264.7 macrophages was quantified following the method described by Erkoc et al. [62]. Briefly, 2×10^4 RAW 264.7 macrophages per well were plated in a 96-well plate and incubated at 37 °C for 24 h. Venom from *D. acutus* at varying concentrations, vehicle (negative control), or 0.1 μg/ml lipopolysaccharide (LPS, positive control) was added to stimulate NO synthesis. Alternatively, cells pre-treated with venom or vehicle for 30 min were exposed to 0.1 μg/ml LPS to assess the inhibition of NO synthesis. After 24 h, supernatants were collected and stored at −80 °C. A standard curve was generated using different concentrations of sodium nitrite (0–3.45 μg/ml). Subsequently, 80 μl of cell supernatant or standard was combined with 20 μl of sulfanilamide solution (40 mg/ml in 1 M HCl) and 20 μl of naphthylene diamine solution (60 mg/ml N-(1-naphthyl)ethylenediamine dihydrochloride in water) and incubated for 15 min. The absorbance at $\lambda = 540$ nm was measured using an EnSpire Plate Reader (Perkin Elmer). Normalisation for the induction assay and the inhibition assay was performed against the positive control (100 %) and against the vehicle/negative control (100 %), respectively.

3. Results

3.1. Composition of the D. acutus venom proteome

In order to explore the biomolecular complexity within *D. acutus* venom, we first carried out a chemical profiling via RP-HPLC and one-dimensional SDS-PAGE. The chromatographic profile was characterised by 10 main peaks, along with several minor ones that were difficult to separate from the background noise and were thus not considered (Fig. 2A). A gradual increase in peak intensity could be detected from peak 3 to peak 10. One-dimensional SDS-PAGE analysis was conducted under both reducing and non-reducing conditions (Fig. 2B). The majority of identified bands are in the range of 13–50 kDa. The gel profiles exhibited a notable absence of prominent bands exceeding 50 kDa in molecular weight, with a single band at 75 kDa. Putative toxin families, including CTL, svMP, svSP, and PLA_2, were assigned to the retrieved bands based on prior *D. acutus* venom SDS-PAGE profiles [39,67].

Following this initial assessment of the *D. acutus* venom profile, we established a comprehensive sequence-level atlas of the species' toxin arsenal. To achieve this, we employed a previously sequenced high-quality sharp-nosed viper genome [44] as a peptide search database for bottom-up shotgun proteomics. Through this approach, we identified a total of 117 proteins in the analysed sample, along with their nucleotide and amino acid sequences (see Tables S1 and S2). Rigorous quality filtering, which included BLAST searches, Interproscan, and manual comparative alignment investigation, allowed us to pinpoint 45 bona fide venom components from 20 protein families, categorised into 18 distinct protein groups (Tables S3 and S4). The most diverse protein family was svSP with nine entries, constituting 20 % of the total number of venom-related components, followed by svMP with six entries (13 %),

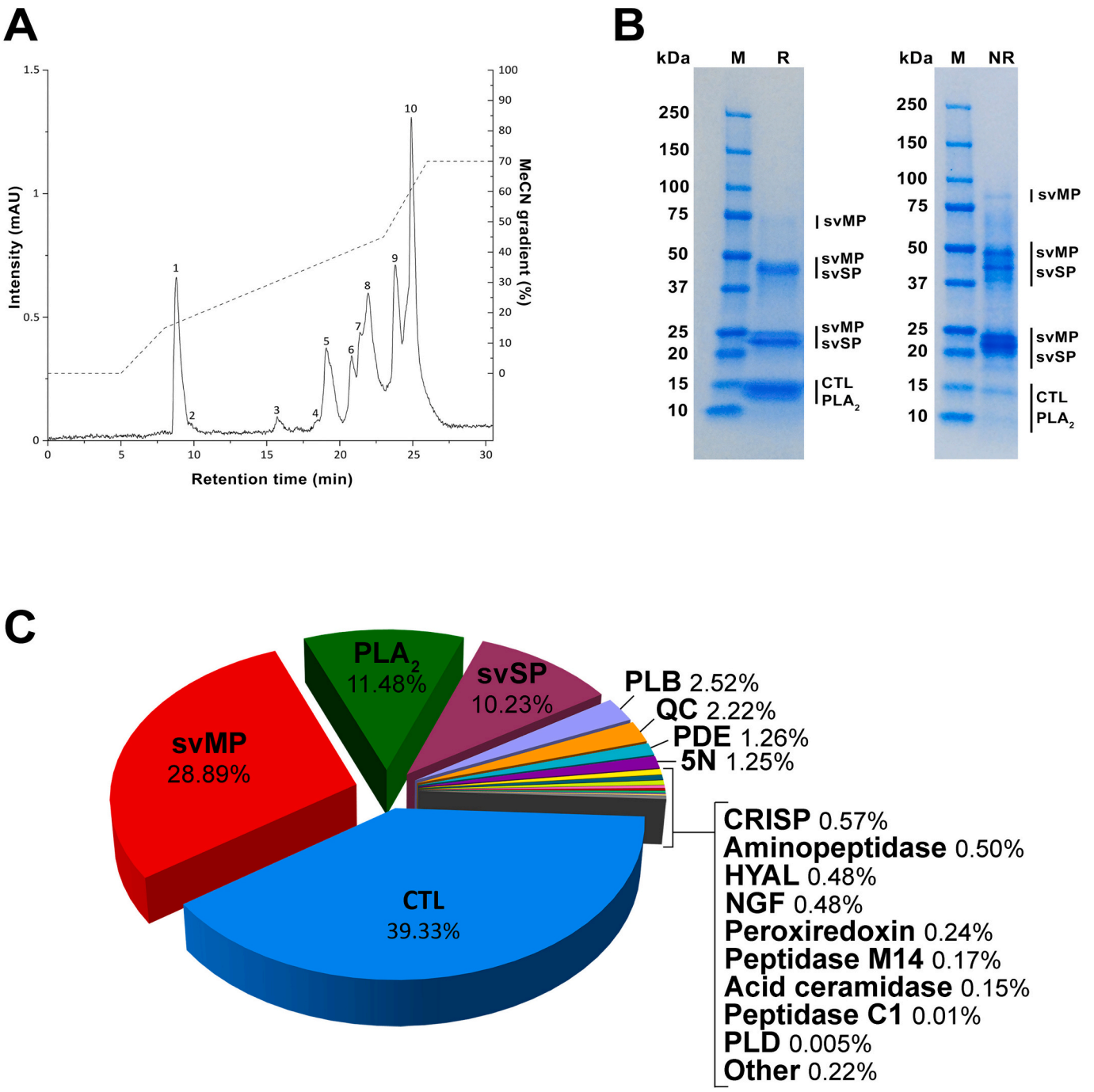

Fig. 2. Characterisation of sharp-nosed viper venom. (A) RP-HPLC profile, (B) one-dimensional SDS-PAGE profiles, and (C) relative abundances of the venom components based on NSAFs are presented. In the SDS-PAGE profiles, putative venom toxin families were assigned based on molecular weight, following Liu et al. [39] and Tsai et al. [67]. Abbreviations: M, marker; NR, non-reduced; R, reduced. Toxin family key: 5N, 5′-nucletotidase; CRISP, cysteine-rich secretory protein; CTL, C-type lectin and C-type lectin-related protein; HYAL, hyaluronidase; NGF, venom nerve growth factor; PDE, phosphodiesterase; PLA_2, phospholipase A_2; PLB, phospholipase B; PLD, phospholipase D; QC, glutaminyl-peptide cyclotransferase; svMP, snake venom metalloproteinase; svSP, snake venom serine protease.

and CTLs with four entries (9 %). Manual sequence analysis revealed that the identified svMPs belong to classes P-II (two entries) and P-III (four entries) (see Table S3). Specifically, the identified P-II svMPs exhibited considerable sequence similarity with metalloproteinases of the adamalysin II-like subfamily, such as jerdonitin [XP_015681821]. The identified P-III svMPs showed the highest sequence similarity with agkihagin [Q1PS45], a potent inhibitor of platelet aggregation isolated from *D. acutus* [68]. The same analysis classified the two detected PLA_2 as members of the D49 subfamily.

To obtain a quantitative perspective on the sharp-nosed viper venom profile, we calculated the NSAF for each component, which represents a reliable estimate of their relative abundance [69,70]. Our analysis revealed that the toxin families CTL, svMP, PLA_2, and svSP presented the highest abundances (39 %, 29 %, 12 %, and 10 %, respectively), accounting for 90 % of the *D. acutus* venom proteome. Additional proteins, accounting together for approximately 7 % of the proteome, were phospholipase B (PLB, 3 %), glutaminyl-peptide cyclotransferase (QC, 2 %), phosphodiesterase (PDE, 1 %), and 5′-nucleotidase (5N, 1 %). Cysteine-rich secretory protein (CRISP), aminopeptidase, hyaluronidase (HYAL), venom nerve growth factor (NGF), peroxiredoxin, peptidase

M14, acid ceramidase, peptidase C1, and phospholipase D (PLD) each accounted for <1 % of the proteome. Finally, five components (i.e., Dacu_04176, Dacu_04177, Dacu_05789, Dacu_07255, and Dacu_09023) with an uncertain PEAKS-based protein group classification were reported as "other", and accounted for approximately 0.2 % of the venom proteome. Additional information on the components identified and their abundances is reported in Fig. 2C and in Tables S3 and S4.

3.2. Bioactivity profiling of sharp-nosed viper venom

Following our proteomic assessment of sharp-nosed viper venom, we aimed to investigate its bioactivity spectrum to functionally contextualise the identified components. To achieve this, we performed a broad array of bioassays targeting typical viper venom activities.

Our proteomic screening of the *D. acutus* venom revealed a range of proteases (svMP and svSP) as well as PLA_2s as the main enzymatic components (Fig. 2). Thus, we measured the general protease and PLA_2 activity exhibited by *D. acutus* venom using photometric assays. The venom showed high levels of protease activity across all tested concentrations, ranging from 38 to 69 % in a concentration-dependent manner (Fig. 3). We observed potent, concentration-dependent effects also for PLA_2 activity, which ranged between 13 % (3.125 μg/ml) and 95 % (50 μg/ml) (Fig. 3).

Potentially fatal effects on the haemostatic system of the envenomated subjects are a characteristic symptom of envenomation by *D. acutus* [31,71,72]. Accordingly, we explored the effects of its venom on different haematological targets. The venom showed weak haemolytic activity under the tested conditions, ranging from 2 % to a maximum of 5 %. While we detected factor Xa activity at 50 μg/ml (12 %), we did not observe any activity at lower concentrations. Thrombin activity ranged from 0.11 % to 8.5 %, and was lower than 1 % at 6.25 μg/ml and 3.125 μg/ml. Increasing venom concentrations resulted in a rise in thrombin activity. No plasmin activity was detected at the tested concentrations.

Other than affecting the haemostatic system, the venom of *D. acutus* is known to cause considerable tissue damage [32,34,72]. Therefore, we investigated its cytotoxicity across five mammalian cell lines of different origin (canine, MDCK II; murine, RAW 264.7; human, A549, HEK 293T, and SH-SY5Y) and primary human peripheral blood mononuclear cells (PBMCs). We observed potent concentration-dependent cytotoxicity in the canine kidney cell line MDCK II and in lung epithelial A549 cells, with generally stronger effects on MDCK II cells (i.e., 16 % vs. 41 % cell viability observed in A549 cells at 25 μg/ml). A positive relationship between concentration and cytotoxicity was also detected for human embryonal kidney cell line HEK 293T and, less markedly, for the human neuroblastoma cell line SH-SY5Y (16 % and 64 % cell viability at concentration 25 μg/ml, respectively). In MDCK II, A549, HEK 293T and SH-SY5Y cells, the most remarkable decrease in viability was observed after treatment with venom at concentration 25 μg/ml. No cytotoxicity of the applied venom concentrations could be detected on human PBMC and murine macrophages (RAW 264.7). Additional information on the cytotoxicity assays is reported in Fig. 4.

Lastly, we aimed to test whether *D. acutus* venom may play a role in influencing cell-cell signalling and causing inflammation. Therefore, we measured its effect on intracellular Ca^{2+} release in HEK 293T and SH-SY5Y cells, and on NO levels in RAW 264.7 cells. No apparent effects of *D. acutus* venom on either of the tested targets were observed. Further

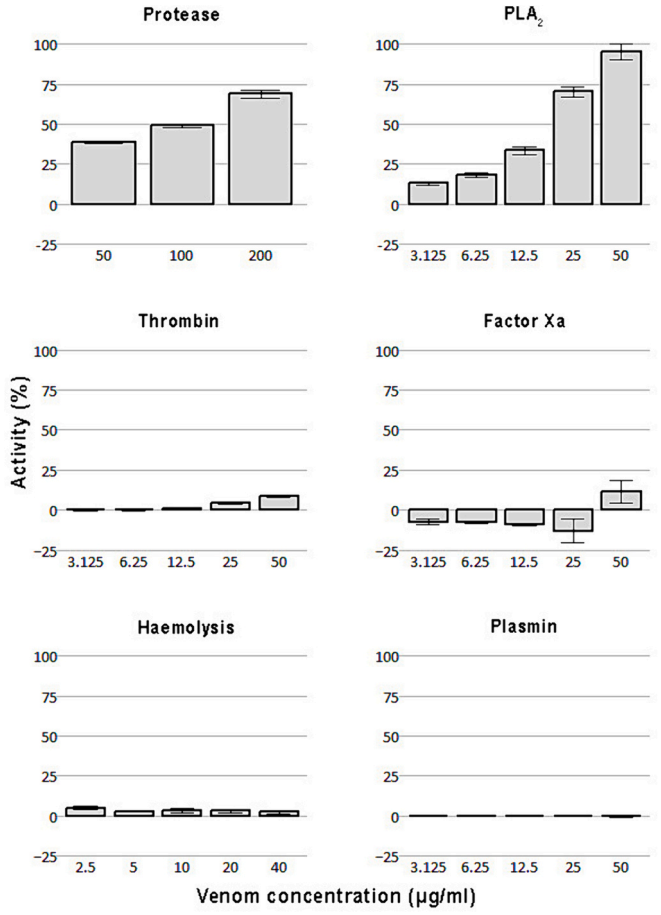

Fig. 3. Biological activity of *D. acutus* venom. The values presented in each graph refer to the normalised averages of the values of at least three measurements per concentration.

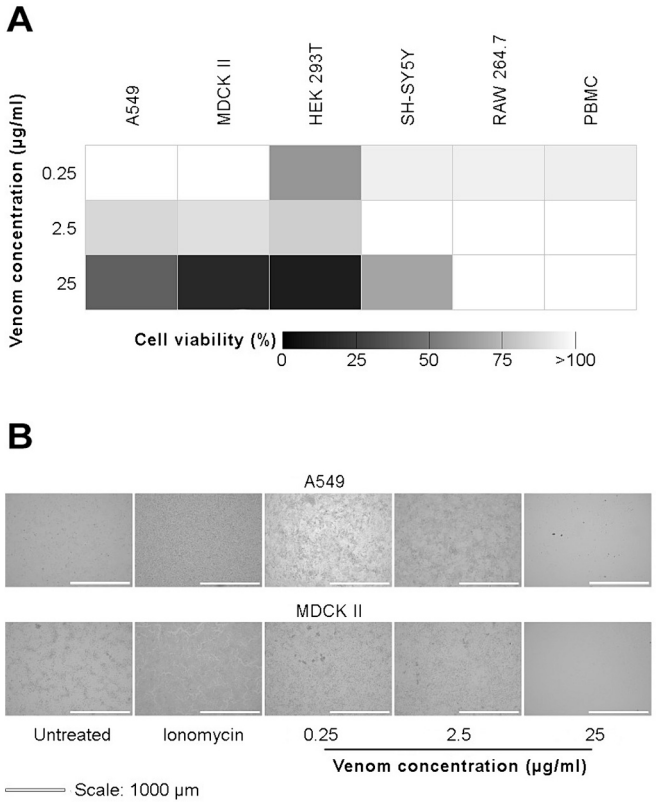

Fig. 4. Cytotoxicity of *D. acutus* venom. (A) Heatmap showing the effect of the analysed venom on the viability of the five tested mammalian cell lines and the PBMCs. (B) Photographs showing the cytotoxic effect of the venom on A549 and MDCK II cells at three different concentrations, with negative (untreated/vehicle ddH_2O) and positive (ionomycin) controls included. Scale bar: 1 mm.

details on the results of all performed bioassays are reported in Tables S5–S14.

4. Discussion

4.1. The first genome-annotated venom proteome of Deinagkistrodon acutus

The implementation of next-generation databases is paramount to overcome some of the primary hurdles inherent to peptide-centric proteomic techniques, including the "missing values problem", referred as inferring proteins based on incomplete sequence coverage [73]. Indeed, shotgun proteomics is generally able to provide a detailed view of the polypeptide diversity of a venom [74], but it is especially powerful when the generated MS data can be aligned with a species-specific omics-derived database, such as a genome or a venom gland transcriptome [22,75]. In light of this, our integrative proteogenomics approach, combining shotgun proteomics with genome-based protein identification of the venom composition of *D. acutus*, likely provides one of the most accurate venom protein catalogues currently available for this species of critical medical importance.

Through proteogenomics, we identified a total of 117 components in the venom of *D. acutus*, many of which were physiological proteins (Table S1). Considering that the functional space in snake venom of the vast majority of physiological proteins remains unknown, they were excluded from further analysis. Therefore, we ultimately considered 45 proteins, and classified them into 18 different groups. Of these, 17 groups comprise well-known snake venom protein families and account for almost the total venom proteome (>99 %, 40 components). The remaining group ("Other") accounts for <0.3 % of the proteome (Fig. 2), and comprises five components potentially playing a role in envenomation (Table S3).

Interestingly, we noticed evident differences in the number of venom-related components yielded by our analysis and those from previous works. For instance, Liu et al. [39] identified 34 components divided into 11 protein groups, Chen et al. [40] 29 proteins from eight protein families, and Qin et al. [42] 97 proteins from six protein families. Differences were also detected when considering the shotgun-proteomics-based works by Nie et al. [76] and Huang et al. [41], reporting 85 proteins (10 groups) and 103 proteins (15 groups), respectively. Despite the qualitative differences mentioned above, our genome-based venomic analysis is overall in line with previous characterisations of *D. acutus* venom. Indeed, our results from proteogenomics, RP-HPLC, and SDS-PAGE profiling, as well as some of the venom proteomes previously published [39,40,42], indicate that the venom of this species is relatively simple, with the four protein families CTL, svMP, svSP, and PLA_2 comprising almost the totality of its composition The high relative abundances of these major protein families are concordant with the symptoms typically associated with envenomation by sharp-nosed vipers, namely haemorrhage, cytotoxicity, and coagulopathy [71,72]. Indeed, svMP (particularly of class P-III) are well-known for their haemorrhagic and tissue-damaging potential [77,78], whereas svSP and CTL mainly influence haemostasis, affecting fibrinolysis and platelet aggregation [79,80], and PLA_2 exhibit a wide range of effects, including cytotoxicity and coagulopathy [81,82].

At a finer scale, however, discrepancies with previous studies can be detected regarding the abundances of the protein families constituting *D. acutus* venom. Based on the abundance of high-intensity, late-eluting RP-HPLC peaks (Fig. 2A), typically associated with high amounts of svMP and CTL [83–86], and the putative classification of the SDS-PAGE bands (Fig. 2B), we expected those to be the most abundant toxin families. In line with our chromatographic and SDS-PAGE profile, but contrary to what is reported in previous works [40,42,76], our NSAF-based quantification indeed revealed CTL as predominant (39 % of the proteome), followed by svMP (29 %; Fig. 2).

In light of the differences mentioned above, it must be noted that the previous studies on the composition of *D. acutus* venom applied different proteomics protocols, making them difficult to compare quantitatively. Furthermore, all previous works exclusively relied on public databases for protein identification. Considering the low specificity of such databases [25], we suspect that the differences between the number of venom components identified through our proteogenomics-based analysis and those previously reported stem from differences in the methodologies applied. Nonetheless, we cannot exclude that these discrepancies may be attributable to intraspecific venom variation, reported at different magnitudes for several viperid snakes [87–89]. Indeed, intraspecific venom variation has been suggested for *D. acutus*, although primarily based on comparative analyses of chromatographic and SDS-PAGE profiles [67,90] and antivenom efficacy [91], and should thus be investigated in further detail through the application of comprehensive omics-based techniques.

4.2. Functional insights into clinical symptoms of D. acutus envenoming

Bites inflicted by *D. acutus* primarily cause symptoms involving significant tissue damage and haemostatic disturbances, including haemorrhage, prolonged coagulation time, hypofibrinogenaemia, and thrombocytopenia [31,32,71,72,92]. These symptoms align with the typical activities exerted by the major venom components identified in our proteogenomics experiment. Similarly, our bioactivity screening targeting several of these effects mirrored the clinical picture typically arising following *D. acutus* envenomation.

The severe tissue damage and haemorrhage contribute significantly to the medical burden imposed by this species [32,34]. Interestingly, *D. acutus* venom has been reported to particularly impair the kidneys and lungs of its victims [41,72]. In light of this, we carried out a broad in vitro screening of *D. acutus* venom across five different mammalian cell lines from various tissues, including lungs, kidneys, neurons, and macrophages, and the primary cells PBMCs. Overall, this screening revealed a general and often potent, concentration-dependent cytotoxicity of *D. acutus* venom, consistent with its powerful tissue-damaging effects.

Our results further show that *D. acutus* venom causes the most potent cytotoxic effects on MDCK II, HEK 293T, and A549 cells (Fig. 4). The high affinity observed for the epithelial-like kidney cells (i.e., MDCK II and HEK 293T) and epithelial lung cells (i.e., A549) is consistent with the reported direct impairment of the kidney and lung caused by sharp-nosed viper envenomation [72,93].

The potent cytotoxic activity displayed by *D. acutus* venom at the highest concentration tested (i.e., 25 μg/ml) may primarily stem from typical viper venom components exerting enzymatic activities, particularly proteases and PLA_2s [94,95]. Indeed, our proteogenomics profiling indicates these as the two major enzymatic classes, comprising approximately 50 % of the NSAF-quantified venom proteome. We recovered high levels of protease and PLA_2 activity, up to 69 % and 95 %, respectively (Fig. 3). Thus, the enzymatic activity assays performed draw a coherent picture, in agreement with the obtained *D. acutus* venom profile, the detected cytotoxicity, and the clinical symptoms typically reported following envenoming by this species.

The cytotoxic and haemorrhagic symptoms induced by the venoms of several snake species are frequently exacerbated by blood clotting disturbances resulting from venom-induced consumption coagulopathy, a disseminated intravascular coagulation-like syndrome causing a broad range of clotting factor deficiencies, ultimately leading to incoagulable blood [96]. Based on the clinical and laboratory evidence indicating that the venom of *D. acutus* exerts an anticoagulant effect on the haemostatic system of the envenomated subjects [32,33,36,37,92], we further investigated the potential of *D. acutus* venom to activate several human blood coagulation factors. Our analysis on factor Xa, plasmin, and thrombin activity revealed low levels of activation potential for these important haemostatic targets, consistent with the activity profile expected from an anticoagulant venom. Although the venom of *D. acutus* is reported to be mainly anticoagulant, some minor procoagulant and

pseudo-procoagulant effects and components have also been detected [33,91,97]. In this context, the low levels of factor Xa and thrombin activity (maximum 12 % and 8.5 %, respectively) and the absence of plasmin activity observed in the performed bioassays could support a possibly (pseudo-)procoagulant nature of the analysed venom (Fig. 3).

5. Conclusion

Snakebite is a major global health burden particularly impacting rural communities from the developing countries of Africa, Asia and Latin America. Comprehensive assessments of venom compositions and venom activities from medically relevant snakes are important weapons for understanding venom pathochemistry, optimising treatment, and developing novel antidotes. The sharp-nosed viper (*Deinagkistrodon acutus*) causes significant tissue damage and potentially fatal haemostatic disturbances, making it one of the snakes of highest medical importance in Asia. Here, we present the most detailed and comprehensive overview to date of the sharp-nosed viper toxin repertoire, derived via RP-HPLC and SDS-PAGE profiling, coupled with the first proteogenomic assessment of its venom. The resulting proteomic profile highlights the venom's relatively simple composition, primarily consisting of four major protein families (i.e., CTL, svMP, svSP, and PLA_2). These findings align with the haemorrhagic, cytotoxic, and coagulopathic symptoms typically associated with envenomation caused by this pit viper. When analysing composition and bioactivity, we detected differences compared to what was reported in previous studies, underscoring the need for further investigation into the sources of this variation. Comparative analyses employing comprehensive omics-based techniques to investigate the venoms from a range of different specimens across populations, sexes, and life history stages would shed light on the extent and functional implications of venom variability within this species.

The detailed insights provided by the combination of proteogenomics with biological assays represent a significant advancement in understanding snake venom composition and exochemistry, as here shown for *D. acutus*. Adopting our workflow and establishing more specific databases, particularly employing high-quality genomes and venom gland transcriptomes, will improve the accuracy of protein identification in venomics studies. Moreover, in vivo studies are essential to validate in vitro findings and explore the systemic effects of the venom in greater detail. Bridging the gap between bench and bedside by integrating toxinology, pharmacology, and clinical medicine is of paramount importance for translating these findings into improved clinical management protocols for *D. acutus* envenomation, ultimately enhancing the outcomes for affected individuals.

CRediT authorship contribution statement

Ignazio Avella: Writing – review & editing, Writing – original draft, Visualization, Supervision, Project administration, Methodology, Investigation, Formal analysis, Data curation, Conceptualization. **Lennart Schulte:** Writing – review & editing, Visualization, Software, Methodology, Investigation, Formal analysis, Data curation. **Sabine Hurka:** Writing – review & editing, Visualization, Software, Methodology, Investigation, Formal analysis, Data curation. **Maik Damm:** Writing – review & editing, Visualization, Investigation, Data curation. **Johanna Eichberg:** Writing – review & editing, Investigation, Formal analysis, Data curation. **Susanne Schiffmann:** Writing – review & editing, Investigation, Formal analysis, Data curation. **Marina Henke:** Investigation, Formal analysis, Data curation. **Thomas Timm:** Writing – review & editing, Software, Resources, Methodology, Investigation, Formal analysis, Data curation. **Günther Lochnit:** Writing – review & editing, Software, Resources, Methodology, Investigation, Formal analysis, Data curation. **Kornelia Hardes:** Writing – review & editing, Resources. **Andreas Vilcinskas:** Writing – review & editing, Supervision, Project administration, Funding acquisition. **Tim Lüddecke:** Writing – review & editing, Visualization, Supervision, Software, Resources, Project administration, Methodology, Investigation, Funding acquisition, Formal analysis, Data curation, Conceptualization.

Declaration of competing interest

The authors declare that they have no known competing financial interests or personal relationships that could have appeared to influence the work reported in this paper.

Acknowledgements

The authors thank Prof. Dr. Eva Böttcher-Friebertshäuser (Institute of Virology, Philipps-University Marburg) and Alejandra Centurión (Pest and Vector Control Department, Fraunhofer Institute for Molecular Biology and Applied Ecology) for providing the MDCK II cells and sheep blood used for the cytotoxicity and haemolytic activity assays, respectively. IA thanks Nahla Lucchini for her assistance with the creation of the map in Fig. 1. Special thanks are extended to Sam Huang and Tom Williams for providing the pictures used to assemble Fig. 1.

Funding sources

TL, LS, and MD were funded by the Deutsche Forschungsgemeinschaft (DFG, German Research Foundation) – 505696476 (TL and LS) and 540833593 (MD). JE and KH were funded by the Bundesministerium für Bildung und Forschung (BMBF, Federal Ministry of Education and Research), grant number 01KI2024. This work was further financially supported via the Hesse Ministry of Sciences and Arts (HMWK) via the LOEWE-Centre for Translational Biodiversity Genomics (LOEWE-TBG) granted to AV and SS. IA gratefully acknowledges the financial support received from the European Cooperation in Science and Technology (COST) through the Action CA19144 EUVEN (ref. E-COST-GRANT-CA19144-9da371bb).

Appendix A. Supplementary data

Supplementary data to this article can be found online at https://doi.org/10.1016/j.ijbiomac.2024.135041.

References

[1] J.P. Chippaux, Snakebite envenomation turns again into a neglected tropical disease!, J. Venom. Anim. Toxins. 23 (2017) 38, https://doi.org/10.1186/s40409-017-0127-6.
[2] A. Kasturiratne, A.R. Wickremasinghe, N. de Silva, N.K. Gunawardena, A. Pathmeswaran, R. Premaratna, L. Savioli, D.G. Lalloo, H.J. de Silva, The global burden of snakebite: a literature analysis and modelling based on regional estimates of envenoming and deaths, PLoS Med. 5 (2008) e218, https://doi.org/10.1371/journal.pmed.0050218.
[3] J.M. Gutiérrez, J.J. Calvete, A.G. Habib, R.A. Harrison, D.J. Williams, D.A. Warrell, Snakebite envenoming, Nat. Rev. Dis. Primers 3 (2017) 1–21, https://doi.org/10.1038/nrdp.2017.63.
[4] A.F.V. Pintor, N. Ray, J. Longbottom, C.A. Bravo-Vega, M. Yousefi, K.A. Murray, D. S. Ediriweera, P.J. Diggle, Addressing the global snakebite crisis with geo-spatial analyses - recent advances and future direction, Toxicon X. 11 (2021) 100076, https://doi.org/10.1016/j.toxcx.2021.100076.
[5] GBD 2019 Snakebite Envenomation Collaborators, Global mortality of snakebite envenoming between 1990 and 2019, Nat. Commun. 13 (2022) 6160, https://doi.org/10.1038/s41467-022-33627-9.
[6] R.A. Harrison, A. Hargreaves, S.C. Wagstaff, B. Faragher, D.G. Lalloo, Snake envenoming: a disease of poverty, PLoS Neglect. Tropical D. 3 (2009) e569, https://doi.org/10.1371/journal.pntd.0000569.
[7] J. Longbottom, F.M. Shearer, M. Devine, G. Alcoba, F. Chappuis, D.J. Weiss, S. E. Ray, N. Ray, D.A. Warrell, R. Ruiz de Castañeda, D.J. Williams, S.I. Hay, D. M. Pigott, Vulnerability to snakebite envenoming: a global mapping of hotspots, Lancet 392 (2018) 673–684, https://doi.org/10.1016/S0140-6736(18)31224-8.
[8] World Health Organization, Snakebite Envenoming. https://www.who.int/news-room/fact-sheets/detail/snakebite-envenoming, 2023 (accessed 10 July 2024).
[9] R. Minghui, M.N. Malecela, E. Cooke, B. Abela-Ridder, WHO's snakebite envenoming strategy for prevention and control, Lancet Glob. Health 7 (2019) e837–e838, https://doi.org/10.1016/S2214-109X(19)30225-6.

[10] N.R. Casewell, T.N. Jackson, A.H. Laustsen, K. Sunagar, Causes and consequences of snake venom variation, Trends Pharmacol. Sci. 41 (2020) 570–581, https://doi.org/10.1016/j.tips.2020.05.006.
[11] D.A. Warrell, Snake bite, Lancet 375 (2010) 77–88, https://doi.org/10.1016/S0140-6736(09)61754-2.
[12] J. Slagboom, J. Kool, R.A. Harrison, N.R. Casewell, Haemotoxic snake venoms: their functional activity, impact on snakebite victims and pharmaceutical promise, Brit. J. Haemat. 177 (2017) 947–959, https://doi.org/10.1111/bjh.14591.
[13] M. Damm, B.F. Hempel, R.D. Süssmuth, Old world vipers—a review about snake venom proteomics of viperinae and their variations, Toxins 13 (2021) 427, https://doi.org/10.3390/toxins13060427.
[14] M.R. Di Nicola, A. Pontara, G.E.N. Kass, N.I. Kramer, I. Avella, R. Pampena, S. R. Mercuri, J.L.M. Dorne, G. Paolino, Vipers of major clinical relevance in Europe: taxonomy, venom composition, toxicology and clinical management of human bites, Toxicology 453 (2021) 152724, https://doi.org/10.1016/j.tox.2021.152724.
[15] J.J. Calvete, Snake venomics: from the inventory of toxins to biology, Toxicon 75 (2013) 44–62, https://doi.org/10.1016/j.toxicon.2013.03.020.
[16] F.J. Fuzita, M.W. Pinkse, J.S. Patane, P.D. Verhaert, A.R. Lopes, High throughput techniques to reveal the molecular physiology and evolution of digestion in spiders, BMC Genomics 17 (2016) 1–19, https://doi.org/10.1186/s12864-016-3048-9.
[17] V. Oldrati, M. Arrell, A. Violette, F. Perret, X. Sprüngli, J.L. Wolfender, R. Stöcklin, Advances in venomics, Mol. BioSyst. 12 (2016) 3530–3543, https://doi.org/10.1039/c6mb00516k.
[18] T. Tasoulis, G.K. Isbister, A review and database of snake venom proteomes, Toxins 9 (2017) 290, https://doi.org/10.3390/toxins9090290.
[19] I. Avella, W. Wüster, L. Luiselli, F. Martínez-Freiría, Toxic habits: an analysis of general trends and biases in snake venom research, Toxins 14 (2022) 884, https://doi.org/10.3390/toxins14120884.
[20] R.K. Brahma, R.J. McCleary, R.M. Kini, R. Doley, Venom gland transcriptomics for identifying, cataloging, and characterizing venom proteins in snakes, Toxicon 93 (2015) 1–10, https://doi.org/10.1016/j.toxicon.2014.10.022.
[21] C.M. Modahl, R.K. Brahma, Snake venom gland transcriptomics, in: S.P. Mackessy (Ed.), Handbook of Venoms and Toxins of Reptiles, second ed., CRC Press, Boca Ratón, 2021, pp. 43–57.
[22] W.Q. Rao, K. Kalogeropoulos, M.E. Allentoft, S. Gopalakrishnan, W.N. Zhao, C. T. Workman, C. Knudsen, B. Jiménez-Mena, L. Seneci, M. Mousavi-Derazmahalleh, T.P. Jenkins, E. Rivera-de-Torre, S.Q. Liu, A.H. Laustsen, The rise of genomics in snake venom research: recent advances and future perspectives, GigaScience 11 (2022) giac024, https://doi.org/10.1093/gigascience/giac024.
[23] K. Sunagar, D. Morgenstern, A.M. Reitzel, Y. Moran, Ecological venomics: how genomics, transcriptomics and proteomics can shed new light on the ecology and evolution of venom, J. Proteome 135 (2016) 62–72, https://doi.org/10.1016/j.jprot.2015.09.015.
[24] S.H. Drukewitz, B.M. von Reumont, The significance of comparative genomics in modern evolutionary venomics, Front. Ecol. Evol. 7 (2019) 163, https://doi.org/10.3389/fevo.2019.00163.
[25] B.M. von Reumont, G. Anderluh, A. Antunes, N. Ayvazyan, D. Beis, F. Caliskan, A. Crnković, M. Damm, S. Dutertre, L. Ellgaard, G. Gajski, H. German, B. Halassy, B.F. Hempel, T. Hucho, N. İğci, M.P. Ikonomopoulou, I. Karbat, M.I. Klapa, I. Koludarov, J. Kool, T. Lüddecke, R. Ben Mansour, M.V. Modica, Y. Moran, A. Nalbantsoy, M.E.P. Ibáñez, A. Panagiotopoulos, E. Reuveny, J.S. Céspedes, A. Sombke, J.M. Surm, E.A.B. Undheim, A. Verdes, G. Zancolli, Modern venomics—current insights, novel methods, and future perspectives in biological and applied animal venom research, GigaScience 11 (2022) giac048, https://doi.org/10.1093/gigascience/giac048.
[26] A. Gumprecht, F. Tillack, N.L. Orlov, A. Captain, S. Ryabov, Asian Pitvipers, Geitje Books, Berlin, 2004.
[27] World Health Organization, Snakebite Information and Data Platform. https://www.who.int/teams/control-of-neglected-tropical-diseases/snakebiteen venoming/snakebite-information-and-data-platform/overview#tab=tab_1, 2020 (accessed 11 December 2023).
[28] P. Li, Z. Zhou, *Deinagkistrodon acutus*, the IUCN Red List of Threatened Species 2021, e.T190644A1955997, 2021, https://doi.org/10.2305/IUCN.UK.2021-3.RLTS.T190644A1955997.en (accessed 30 September 2023).
[29] Y.C. Mao, D.Z. Hung, Epidemiology of snake envenomation in Taiwan, in: P. Gopalakrishnakone, A. Faiz, R. Fernando, C. Gnanathasan, A. Habib, C.C. Yang (Eds.), Clinical Toxinology in Asia Pacific and Africa, Toxinology vol. 2, Springer, Dodrecht, 2015, pp. 3–22.
[30] E. Zhao, Venomous snakes of China, in: P. Gopalakrishnakone, L.M. Chou (Eds.), Snakes of Medical Importance (Asia-Pacific Region), Venom and Toxin Research Group, National University of Singapore, Singapore, 1990, pp. 243–268.
[31] Q.B. Li, Q.S. Yu, G.W. Huang, Y. Tokeshi, M. Nakamura, K. Kinjoh, T. Kosugi, Hemostatic disturbances observed in patients with snakebite in south China, Toxicon 38 (2000) 1355–1366, https://doi.org/10.1016/s0041-0101(99)00092-6.
[32] C.L. Cheng, Y.C. Mao, P.Y. Liu, L.C. Chiang, S.C. Liao, C.C. Yang, *Deinagkistrodon acutus envenomation*: a report of three cases, J. Venom. Anim. Toxins. 23 (2017) 20, https://doi.org/10.1186/s40409-017-0111-1.
[33] J. Debono, M.H.A. Bos, F. Coimbra, L. Ge, N. Frank, H.F. Kwok, B.G. Fry, Basal but divergent: clinical implications of differential coagulotoxicity in a clade of Asian vipers, Toxicol. in Vitro 58 (2019) 195–206, https://doi.org/10.1016/j.tiv.2019.03.038.
[34] W. Linfeng, X. Lutao, L. Pin, L. Linjie, C. Meisong, D. Wang, Radial artery aneurysm formation and spontaneous rupture after snake bite to the right forearm, Toxicon 181 (2020) 79–81, https://doi.org/10.1016/j.toxicon.2020.04.098.
[35] C. Ouyang, T.F. Huang, Purification and characterization of the fibrinolytic principle of *Agkistrodon acutus* venom, Biochim. Biophys. Acta 439 (1976) 146–153, https://doi.org/10.1016/0005-2795(76)90170-7.
[36] B. Ding, Z. Xu, C. Qian, F. Jiang, X. Ding, Y. Ruan, Z. Ding, Y. Fan, Antiplatelet aggregation and antithrombosis efficiency of peptides in the snake venom of *Deinagkistrodon acutus*: isolation, identification, and evaluation, Evid-Based Compl. Alt. 2015 (2015) 412841, https://doi.org/10.1155/2015/412841.
[37] J. Huang, W. Song, H. Hua, X. Yin, F. Huang, R.N. Alolga, Antithrombotic and anticoagulant effects of a novel protein isolated from the venom of the *Deinagkistrodon acutus* snake, Biomed. Pharmacother. 138 (2021) 111527, https://doi.org/10.1016/j.biopha.2021.111527.
[38] B.D. Chan, W.Y. Wong, M.M. Lee, P.Y. Yue, X. Dai, K.W. Tsim, W.W. Hsiao, M. Li, X.Y. Li, W.C. Tai, Isolation and characterization of ZK002, a novel dual function snake venom protein from *Deinagkistrodon acutus* with anti-angiogenic and anti-inflammatory properties, Front. Pharmacol. 14 (2023) 1227962, https://doi.org/10.3389/fphar.2023.1227962.
[39] C.C. Liu, C.C. Lin, Y.C. Hsiao, P.J. Wang, J.S. Yu, Proteomic characterization of six Taiwanese snake venoms: identification of species-specific proteins and development of a SISCAPA-MRM assay for cobra venom factors, J. Proteome 187 (2018) 59–68, https://doi.org/10.1016/j.jprot.2018.06.003.
[40] P.C. Chen, M.N. Huang, J.F. Chang, C.C. Liu, C.K. Chen, C.H. Hsieh, Snake venom proteome and immuno-profiling of the hundred-pace viper, *Deinagkistrodon acutus*, in Taiwan, Acta Trop. 189 (2019) 137–144, https://doi.org/10.1016/j.actatropica.2018.09.017.
[41] J. Huang, M. Zhao, C. Xue, J. Liang, F. Huang, Analysis of the composition of *Deinagkistrodon acutus* snake venom based on proteomics, and its antithrombotic activity and toxicity studies, Molecules 27 (2022) 2229, https://doi.org/10.3390/molecules27072229.
[42] W.G. Qin, Z.P. Zhuo, H. Hu, M. Lay, Q.Q. Li, J.T. Huang, L.B. Zeng, Z.J. Liang, F. Long, Q. Liang, Proteomic characteristics of six snake venoms from the Viperidae and Elapidae families in China and their relation to local tissue necrosis, Toxicon 235 (2023) 107317, https://doi.org/10.1016/j.toxicon.2023.107317.
[43] B. Zhang, Q. Liu, W. Yin, X. Zhang, Y. Huang, Y. Luo, P. Qiu, X. Su, J. Yu, S. Hu, G. Yan, Transcriptome analysis of *Deinagkistrodon acutus* venomous gland focusing on cellular structure and functional aspects using expressed sequence tags, BMC Genomics 7 (2006) 152, https://doi.org/10.1186/1471-2164-7-152.
[44] W. Yin, Z.J. Wang, Q.Y. Li, J.M. Lian, Y. Zhou, B.Z. Lu, L.J. Jin, P.X. Qiu, P. Zhang, W.B. Zhu, B. Wen, Y.J. Huang, Z.L. Lin, B.T. Qiu, X.W. Su, H.M. Yang, G.J. Zhang, G.M. Yan, Q. Zhou, Evolutionary trajectories of snake genes and genomes revealed by comparative analyses of five-pacer viper, Nature Comm. 7 (2016) 13107, https://doi.org/10.1038/ncomms13107.
[45] X. Wang, L. Liu, W. Zhu, S. Wang, M. Shi, S. Yang, H. Lu, J. Cao, Genome assembly and annotation of the sharp-nosed pit viper *Deinagkistrodon acutus* based on next-generation sequencing data, GigaByte 2023 (2023) gigabyte88, https://doi.org/10.46471/gigabyte.88.
[46] J.D. Jaffe, H.C. Berg, G.M. Church, Proteogenomic mapping as a complementary method to perform genome annotation, Proteomics 4 (2004) 59–77, https://doi.org/10.1002/pmic.200300511.
[47] A.I. Nesvizhskii, Proteogenomics: concepts, applications and computational strategies, Nat. Methods 11 (2014) 1114–1125, https://doi.org/10.1038/nmeth.3144.
[48] S. Hurka, K. Brinkrolf, R. Özbek, F. Förster, A. Billion, J. Heep, T. Timm, G. Lochnit, A. Vilcinskas, T. Lüddecke, Venomics of the central European myrmicine ants *Myrmica rubra* and *Myrmica ruginodis*, Toxins 14 (2022) 358, https://doi.org/10.3390/toxins14050358.
[49] L. Schulte, M. Damm, I. Avella, L. Uhrig, P. Erkoc, S. Schiffmann, R. Fürst, T. Timm, G. Lochnit, A. Vilcinskas, T. Lüddecke, Venomics of the Milos viper (*Macrovipera schweizeri*) unveils patterns of venom composition and exochemistry across blunt-nosed viper venoms, Front. Mol. Biosci. 10 (2023) 1254058, https://doi.org/10.3389/fmolb.2023.1254058.
[50] B. Buchfink, C. Xie, D.H. Huson, Fast and sensitive protein alignment using DIAMOND, Nat. Methods 12 (2015) 59–60, https://doi.org/10.1038/nmeth.3176.
[51] UniProt Consortium, UniProt: a worldwide hub of protein knowledge, Nucleic Acids Res. 47 (2019) D506–D515, https://doi.org/10.1093/nar/gky1049.
[52] S. Henikoff, J.G. Henikoff, Amino acid substitution matrices from protein blocks, Proc. Natl. Acad. Sci. USA 89 (1992) 10915–10919, https://doi.org/10.1073/pnas.89.22.10915.
[53] P.J. Cock, T. Antao, J.T. Chang, B.A. Chapman, C.J. Cox, A. Dalke, I. Friedberg, T. Hamelryck, F. Kauff, B. Wilczynski, M.J. de Hoon, Biopython: freely available Python tools for computational molecular biology and bioinformatics, Bioinformatics 25 (2009) 1422–1423, https://doi.org/10.1093/bioinformatics/btp163.
[54] F. Teufel, J.J. Almagro Armenteros, A.R. Johansen, M.H. Gíslason, S.I. Pihl, K. D. Tsirigos, O. Winther, S. Brunak, G. von Heijne, H. Nielsen, SignalP 6.0 predicts all five types of signal peptides using protein language models, Nat. Biotechnol. 40 (2022) 1023–1025, https://doi.org/10.1038/s41587-021-01156-3.
[55] N.J. Mulder, R. Apweiler, The InterPro database and tools for protein domain analysis, Curr. Protoc. Bioinformatics 2 (2008) 2–7, https://doi.org/10.1002/0471250953.bi0207s21.
[56] H. Liu, R.G. Sadygov, J.R. III Yates, A model for random sampling and estimation of relative protein abundance in shotgun proteomics, Anal. Chem. 76 (2004) 4193–4201, https://doi.org/10.1021/ac0498563.
[57] B. Zybailov, M.K. Coleman, L. Florens, M.P. Washburn, Correlation of relative abundance ratios derived from peptide ion chromatograms and spectrum counting for quantitative proteomic analysis using stable isotope labeling, Anal. Chem. 77 (2005) 6218–6224, https://doi.org/10.1021/ac050846r.

[58] L. Florens, M.J. Carozza, S.K. Swanson, M. Fournier, M.K. Coleman, J.L. Workman, M.P. Washburn, Analyzing chromatin remodeling complexes using shotgun proteomics and normalized spectral abundance factors, Methods 40 (2006) 303–311, https://doi.org/10.1016/j.ymeth.2006.07.028.
[59] B. Zybailov, A.L. Mosley, M.E. Sardiu, M.K. Coleman, L. Florens, M.P. Washburn, Statistical analysis of membrane proteome expression changes in *Saccharomyces cerevisiae*, J. Proteome Res. 5 (2006) 2339–2347, https://doi.org/10.1021/pr060161n.
[60] I. Avella, L. Schulte, M. Damm, T. Timm, G. Lochnit, T. Lüddecke, DATASET - mass spectrometry - snake venom proteomics of *Deinagkistrodon acutus* [dataset], Zenodo (2024), https://doi.org/10.5281/zenodo.12785576.
[61] S. Hurka, T. Lüddecke, A. Paas, L. Dersch, L. Schulte, J. Eichberg, K. Hardes, K. Brinkrolf, A. Vilcinskas, Bioactivity profiling of in silico predicted linear toxins from the ants *Myrmica rubra* and *Myrmica ruginodis*, Toxins 14 (2022) 846, https://doi.org/10.3390/toxins14120846.
[62] P. Erkoc, S. Schiffmann, T. Ulshöfer, M. Henke, M. Marner, J. Krämer, R. Predel, T. F. Schäberle, S. Hurka, L. Dersch, A. Vilcinskas, R. Fürst, T. Lüddecke, Determining the pharmacological potential and biological role of linear pseudoscorpion toxins via functional profiling, iScience 27 (2024) 110309, https://doi.org/10.1016/j.isci.2024.110209.
[63] K.B.M. Still, J. Slagboom, S. Kidwai, C. Xie, Y. Zhao, B. Eisses, Z. Jiang, F.J. Vonk, G.W. Somsen, N.R. Casewell, J. Kool, Development of high-throughput screening assays for profiling snake venom phospholipase A_2 activity after chromatographic fractionation, Toxicon 184 (2020) 28–38, https://doi.org/10.1016/j.toxicon.2020.05.022.
[64] I.P. Sæbø, M. Bjørås, H. Franzyk, E. Helgesen, J.A. Booth, Optimization of the hemolysis assay for the assessment of cytotoxicity, Int. J. Mol. Sci. 24 (2023) 2914, https://doi.org/10.3390/ijms24032914.
[65] A. Galione, G.C. Churchill, Interactions between calcium release pathways: multiple messengers and multiple stores, Cell Calcium 32 (2002) 343–354, https://doi.org/10.1016/s0143416002001902.
[66] C. Bogdan, Nitric oxide and the immune response, Nat. Immunol. 2 (2001) 907–916, https://doi.org/10.1038/ni1001-907.
[67] T.S. Tsai, I.H. Tsai, J.L. Qiu, Y.Y. Chan, Y.W. Chiang, Comparative analysis of *Deinagkistrodon acutus* venom from Taiwan and China utilizing chromatographic, electrophoretic, and bioinformatic approaches, along with ELISA employing a monospecific antivenom, Toxicon 241 (2024) 107663, https://doi.org/10.1016/j.toxicon.2024.107663.
[68] Q. Liu, S. Hu, W. Yin, X. Su, X. Zhang, C. Li, P. Qiu, G. Yan, Construction of a cDNA library from *Agkistrodon acutus* venom gland and identification of Agkihagin, a novel transcript for metalloproteinase, Chinese J. Pharm. T. 20 (2006) 81–90.
[69] A. Chapeaurouge, A. Silva, P. Carvalho, R.J.R. McCleary, C.M. Modahl, J. Perales, R.M. Kini, S.P. Mackessy, Proteomic deep mining the venom of the red-headed krait, *Bungarus flaviceps*, Toxins 10 (2018) 373, https://doi.org/10.3390/toxins10090373.
[70] C.M. Modahl, A.J. Saviola, S.P. Mackessy, Integration of transcriptomic and proteomic approaches for snake venom profiling, Expert Rev. Proteomic. 18 (2021) 827–834, https://doi.org/10.1080/14789450.2021.1995357.
[71] H.Y. Su, S.W. Huang, Y.C. Mao, M.W. Liu, K.H. Lee, P.F. Lai, M.J. Tsai, Clinical and laboratory features distinguishing between *Deinagkistrodon acutus* and *Daboia siamensis* envenomation, J. Venom. Anim. Toxins. 24 (2018) 43, https://doi.org/10.1186/s40409-018-0179-2.
[72] F. Huang, S. Zhao, F. Tong, Y. Liang, J.M. Le Grange, W. Kuang, Y. Zhou, Unexpected death in a young man associated with a unilateral swollen leg: pathological and toxicological findings in a fatal snakebite from *Deinagkistrodon acutus* (Chinese moccasin), J. Forensic Sci. 66 (2021) 786–792, https://doi.org/10.1111/1556-4029.14622.
[73] J.J. Calvete, Snake venomics - from low-resolution toxin-pattern recognition to toxin-resolved venom proteomes with absolute quantification, Expert Rev. Proteomic. 15 (2018) 555–568, https://doi.org/10.1080/14789450.2018.1500904.
[74] J. Slagboom, C. Kaal, A. Arrahman, F.J. Vonk, G.W. Somsen, J.J. Calvete, W. W. Wüster, J. Kool, Analytical strategies in venomics, Microchem. J. 175 (2022) 107187, https://doi.org/10.1016/j.microc.2022.107187.
[75] A.A. Walker, S.D. Robinson, B.F. Hamilton, E.A.B. Undheim, G.F. King, Deadly proteomes: a practical guide to proteotranscriptomics of animal venoms, Proteomics 20 (2020) e1900324, https://doi.org/10.1002/pmic.201900324.
[76] X. Nie, Q. He, B. Zhou, D. Huang, J. Chen, Q. Chen, S. Yang, X. Yu, Exploring the five-paced viper (*Deinagkistrodon acutus*) venom proteome by integrating a combinatorial peptide ligand library approach with shotgun LC-MS/MS, J. Venom. Anim. Toxins. 27 (2021) e20200196, https://doi.org/10.1590/1678-9199-JVATITD-2020-0196.
[77] O.H.P. Ramos, H.S. Selistre-de-Araujo, Snake venom metalloproteases—structure and function of catalytic and disintegrin domains, Comp. Biochem. Physiol. C 142 (2006) 328–346, https://doi.org/10.1016/j.cbpc.2005.11.005.
[78] J.M. Gutiérrez, A. Rucavado, T. Escalante, Snake venom metalloproteinases: biological roles and participation in the pathophysiology of envenomation, in: S. P. Mackessy (Ed.), Evolution of Venomous Animals and Their Toxins, first ed., CRC Press, Boca Ratón, 2010, pp. 115–130.
[79] R.M. Kini, Serine proteases affecting blood coagulation and fibrinolysis from snake venoms, Pathophysiol. Haemo. T. 34 (2005) 200–204, https://doi.org/10.1159/000092424.
[80] J.A. Eble, Structurally robust and functionally highly versatile-C-type lectin (-related) proteins in snake venoms, Toxins 11 (2019) 136, https://doi.org/10.3390/toxins11030136.
[81] H. Xiao, H. Pan, K. Liao, M. Yang, C. Huang, Snake venom PLA_2, a promising target for broad-spectrum antivenom drug development, Biomed. Res. Int. 2017 (2017) 6592820, https://doi.org/10.1155/2017/6592820.
[82] J. Castro-Amorim, A. Novo de Oliveira, S.L. Da Silva, A.M. Soares, A.K. Mukherjee, M.J. Ramos, P.A. Fernandes, Catalytically active snake venom PLA_2 enzymes: an overview of its elusive mechanisms of reaction, J. Med. Chem. 66 (2023) 5364–5376, https://doi.org/10.1021/acs.jmedchem.3c00097.
[83] D. Mora-Obando, J.A. Guerrero-Vargas, R. Prieto-Sánchez, J. Beltrán, A. Rucavado, M. Sasa, J.M. Gutiérrez, S. Ayerbe, B. Lomonte, Proteomic and functional profiling of the venom of *Bothrops ayerbei* from Cauca, Colombia, reveals striking interspecific variation with *Bothrops asper* venom, J. Proteome 96 (2014) 159–172, https://doi.org/10.1016/j.jprot.2013.11.005.
[84] D. Pla, L. Sanz, G. Whiteley, S.C. Wagstaff, R.A. Harrison, N.R. Casewell, J. J. Calvete, What killed Karl Patterson Schmidt? Combined venom gland transcriptomic, venomic and antivenomic analysis of the South African green tree snake (the boomslang), *Dispholidus typus*, BBA-Gen. Subjects 2017 (1861) 814–823, https://doi.org/10.1016/j.bbagen.2017.01.020.
[85] I. Avella, J.J. Calvete, L. Sanz, W. Wüster, F. Licata, S. Quesada-Bernat, Y. Rodríguez, F. Martínez-Freiría, Interpopulational variation and ontogenetic shift in the venom composition of Lataste's viper (*Vipera latastei*, Boscá 1878) from northern Portugal, J. Proteome 263 (2022) 104613, https://doi.org/10.1016/j.jprot.2022.104613.
[86] M. Damm, M. Karış, D. Petras, A. Nalbantsoy, B. Göçmen, R.D. Süssmuth, Venomics and Peptidomics of Palearctic vipers: Clade-wide analysis of seven taxa of the genera *Vipera*, *Montivipera*, *Macrovipera* and *Daboia* across Türkiye, J. Proteome Res. (2024), https://doi.org/10.1021/acs.jproteome.4c00171.
[87] G. Zancolli, J.J. Calvete, M.D. Cardwell, H.W. Greene, W.K. Hayes, M.J. Hegarty, H.W. Herrmann, A.T. Holycross, D.I. Lannutti, J.F. Mulley, L. Sanz, Z.D. Travis, J. R. Whorley, C.E. Wüster, W. Wüster, When one phenotype is not enough: divergent evolutionary trajectories govern venom variation in a widespread rattlesnake species, Proc. R. Soc. Ser. B-Bio. 286 (2019) 20182735, https://doi.org/10.1098/rspb.2018.2735.
[88] I. Avella, M. Damm, I. Freitas, W. Wüster, N. Lucchini, Ó. Zuazo, R.D. Süssmuth, F. Martínez-Freiría, One size fits all-venomics of the Iberian adder (*Vipera seoanei*, Lataste 1878) reveals low levels of venom variation across its distributional range, Toxins 15 (2023) 371, https://doi.org/10.3390/toxins15060371.
[89] M. Damm, I. Avella, R. Merzara, N. Lucchini, J. Buldain, F. Corga, A. Bouazza, S. Fahd, R.D. Süssmuth, F. Martínez-Freiría, Venom variation among the three subspecies of the North African mountain viper *Vipera monticola* (Saint-Girons 1954), Biochimie (2024), https://doi.org/10.1016/j.biochi.2024.07.008.
[90] J.F. Gao, Y.F. Qu, X.Q. Zhang, X. Ji, Within-clutch variation in venoms from hatchlings of *Deinagkistrodon acutus* (Viperidae), Toxicon 57 (2011) 970–977, https://doi.org/10.1016/j.toxicon.2011.03.019.
[91] K.Y. Tan, N.N. Shamsuddin, C.H. Tan, Sharp-nosed pit viper (*Deinagkistrodon acutus*) from Taiwan and China: a comparative study on venom toxicity and neutralization by two specific antivenoms across the strait, Acta Trop. 232 (2022) 106495, https://doi.org/10.1016/j.actatropica.2022.106495.
[92] J. Valenta, Z. Stach, P. Michálek, Envenoming by Crotalid snake Chinese moccasin *Agkistrodon acutus* bite – a case report, Prague Med. Rep. 116 (2015) 155–160, https://doi.org/10.14712/23362936.2015.53.
[93] M. Zhang, J. Cheng, Z. Sun, H. Kong, Y. Zhang, S. Wang, X. Wang, Y. Zhao, H. Qu, Protective effects of carbon dots derived from phellodendri chinensis cortex carbonisata against *Deinagkistrodon acutus* venom-induced acute kidney injury, Nanoscale Res. Lett. 14 (2019) 377, https://doi.org/10.1186/s11671-019-3198-1.
[94] S.E. Gasanov, R.K. Dagda, E.D. Rael, Snake venom cytotoxins, phospholipase A_2s, and Zn^{2+}-dependent metalloproteinases: mechanisms of action and pharmacological relevance, J. Clin. Toxicol. 4 (2014) 1000181, https://doi.org/10.4172/2161-0495.1000181.
[95] J.J. Hiu, M.K.K. Yap, Cytotoxicity of snake venom enzymatic toxins: phospholipase A_2 and L-amino acid oxidase, Biochem. Soc. T. 48 (2020) 719–731, https://doi.org/10.1042/BST20200110.
[96] K. Maduwage, G.K. Isbister, Current treatment for venom-induced consumption coagulopathy resulting from snakebite, PLoS Neglect. Tropical D. 8 (2014) e3220, https://doi.org/10.1371/journal.pntd.0003220.
[97] S.S. Tang, X.H. Wang, J.H. Zhang, B.S. Tang, L. Qian, P.Y. Li, L.W. Luo, Biochemical properties and comparative pharmacology of a coagulant from *Deinagkistrodon acutus* snake venom, Eur. J. Pharm. Sci. 49 (2013) 90–98, https://doi.org/10.1016/j.ejps.2013.02.002.